Using synchrotron high-resolution powder X-ray diffraction for the structure determination of a new cocrystal formed by two active principle ingredients

Mathieu Guerain, Natalia T. Correia, Luisa-Viviane Roca Paixao, Hubert Chevreau, Frédéric Affouard

STRUCTURAL CHEMISTRY

ISSN 2053-2296

Using synchrotron high-resolution powder X-ray diffraction for the structure determination of a new cocrystal formed by two active principle ingredients

Mathieu Guerain,[a]* Natalia T. Correia,[a] Luisa Roca-Paixão,[a] Hubert Chevreau[b] and Frederic Affouard[a]

[a]Université de Lille, CNRS, INRAE, Centrale Lille, UMR 8207-UMET-Unité Matériaux et Transformations, F-59000 Lille, France, and [b]Synchrotron SOLEIL, L Orme des Merisiers, Saint-Aubin, BP 48, 91192 Gif-sur-Yvette, France. *Correspondence e-mail: mathieu.guerain@univ-lille.fr

Received 20 November 2023
Accepted 18 January 2024

Edited by T. Ohhara, J-PARC Center, Japan Atomic Energy Agency, Japan

Keywords: powder diffraction; API; carbamazepine; naproxen; cocrystal; PXRD; crystal structure; liquid-assisted grinding.

CCDC reference: 2327306

Supporting information: this article has supporting information at journals.iucr.org/c

The crystal structure of a new 1:1 cocrystal of carbamazepine and *S*-naproxen ($C_{15}H_{12}N_2O{\cdot}C_{14}H_{14}O_3$) was solved from powder X-ray diffraction (PXRD). The PXRD pattern was measured at the high-resolution beamline CRISTAL at synchrotron SOLEIL (France). The structure was solved using Monte Carlo simulated annealing, then refined with Rietveld refinement. The positions of the H atoms were obtained from density functional theory (DFT) ground-state calculations. The symmetry is orthorhombic with the space group $P2_12_12_1$ (No. 19) and the following lattice parameters: a = 33.5486 (9), b = 26.4223 (6), c = 5.3651 (10) Å and V = 4755.83 (19) Å^3.

1. Introduction

In recent years, the design of functional pharmaceutical molecular materials by the cocrystallization technique has attracted increasing interest (Friščić & Jones, 2010) when other classical approaches based, for example, on salt formation or metastable polymorphs are not possible. The strong development of this strategy has the consequence that many new active pharmaceutical ingredients (APIs) synthesized in the crystalline state exhibit poor solubility and bioavailability that is a major roadblock for pharmaceutical development. The aim is to construct an assembly of neutral multiple chemical species, in a stoichiometric ratio, in the same crystal lattice *via* weak supramolecular interactions of various natures, such as van der Waals, hydrogen, halogen or π–π bonds. These multicomponent materials in the crystalline solid state have an obvious interest in terms of stability, but also in improving many physicochemical properties of an API, such as its aqueous solubility, dissolution, hygroscopicity or bioavailability. Up to now, pharmaceutical cocrystals generally consist of an API and a coformer present in the same crystal lattice (Friščić & Jones, 2010; Vishweshwar *et al.*, 2006; Schultheiss & Newman, 2009; Brittain, 2013; Childs *et al.*, 2009), for example, paracetamol–piperazine (Oswald *et al.*, 2002), ibuprofen–nicotinamide (Berry *et al.*, 2008), carbamazepine–saccharin (Fleischman *et al.*, 2003), carbamazepine–tartaric acid (Guerain *et al.*, 2020), *etc*. In general, the coformer is not an API. In certain cases that are still quite rare, two APIs can be combined (Drozd *et al.*, 2017; Thakuria & Sarma, 2018), a situation which is of obvious interest for multi-therapy approaches.

Carbamazepine (CBZ, $C_{15}H_{12}N_2O$, see Scheme 1), an API used as an anti-epileptic and analgesic drug, is a very common

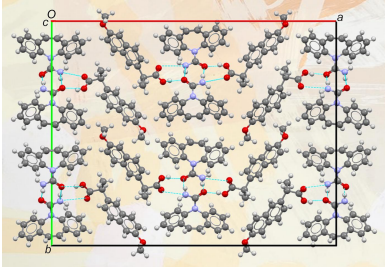

model system for the study of crystallization and cocrystallization (Childs *et al.*, 2009). CBZ is characterized by a rich polymorphism and five anhydrous crystalline forms (Grzesiak *et al.*, 2003; Rustichelli *et al.*, 2000; Arlin *et al.*, 2011) have been reported in the literature. The structure of the stable phase at ambient temperature and atmospheric pressure, named Form III [CBZ(III)], is the commercial form. It is monoclinic with the space group $P2_1/n$ and the following lattice parameters (Eccles *et al.*, 2011): a = 7.55, b = 11.186, c = 13.954 Å and β = 92.938°.

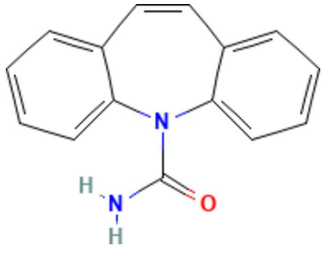

Carbamazepine

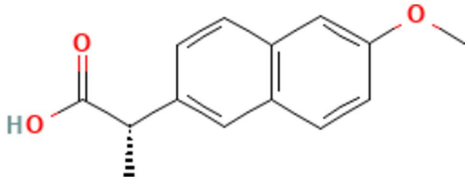

S-Naproxen

Scheme 1

Due to its high polymorphism, and the hydrogen-bonding group offering the possibility of dimer formation, CBZ is also an excellent candidate for cocrystallization, as well as hydrate or solvate formation, as shown by examples in the literature (Vishweshwar *et al.*, 2006; Schultheiss & Newman, 2009; Childs *et al.*, 2009; Guerain *et al.*, 2020; Roca-Paixão *et al.*, 2019; Surov, Ramazanova *et al.*, 2023; Surov, Drozd *et al.*, 2023).

Naproxen (NAP, $C_{14}H_{14}O_3$, see Scheme 1) is a nonsteroidal anti-inflammatory drug (NSAID) used to treat pain, menstrual cramps, inflammatory diseases, such as rheumatoid arthritis, gout and fever. The commercial form of *S*-naproxen (*S*-NAP) is the only known crystallographic form in the literature. It is monoclinic with the space group $P2_1$ and the following lattice parameters (Tang *et al.*, 2015): a = 7.876, b = 5.783, c = 13.323 Å and β = 93.88°. *S*-NAP can form cocrystals with nicotinamide (Ando *et al.*, 2012; Neurohr *et al.*, 2015), isonicotinamide (Castro *et al.*, 2011) and proline (Tilborg *et al.*, 2013; Tumanova *et al.*, 2018), such molecules being generally considered as safe.

In the present study it is shown that a cocrystal of CBZ and *S*-NAP (CBZ:*S*-NAP) can be been obtained from liquid-assisted grinding. It has been verified by coupling the search/match functionalities of *Highscore* software (Degen *et al.*, 2014) with the Cambridge Structural Database (CSD; Groom *et al.*, 2016), the Crystallographic Open Database (COD) (Gražulis *et al.*, 2009) and the PDF-2 database of the International Center for Diffraction Data (ICDD) (Gates-Rector & Blanton, 2019), that this cocrystal has not been referenced in the literature.

A pharmaceutical composition that combines naproxen and carbamazepine is referred to in patent EA200200910 (A1) (Coe *et al.*, 2003; *A pharmaceutical composition for treatment of acute, chronic pain and/or neuropathic pain and migraines*), but no reference is made to the elaboration of a cocrystal.

The present article aims to resolve the structure of the cocrystal CBZ:*S*-NAP obtained by liquid-assisted grinding in a 1:1 molar ratio. The structure was solved *ab initio* from powder X-ray diffraction using a direct-space approach (simulated annealing) and refined by the Rietveld method. The positions of the H atoms were estimated from energy minimization simulation.

2. Experimental

2.1. Cocrystal synthesis

S-Naproxen (purity higher than 98%) was purchased from Sigma–Aldrich and the material was used without any purification. The analysis of the powder X-ray diffraction pattern has shown that the commercial material is in the stable monoclinic phase (CSD refcode COYRUD13; Tang *et al.*, 2015).

Carbamazepine (purity 99.8%) was purchased from Duchefa Farma BV and the material was used without any purification. The analysis of the powder X-ray diffraction pattern has shown that the commercial material is in the stable monoclinic phase (CSD refcode CBMZPN14; Eccles *et al.*, 2011).

The cocrystal was obtained by liquid-assisted grinding of 200 mg of a mixture of CBZ and *S*-NAP, in a 1:1 molar ratio, at 30 Hz for a period of 30 min, adding 20 µl of methanol to the mixture (Roca-Paixão *et al.*, 2019). Differential scanning calorimetry (DSC, Q1000, TA Instruments) reveals a single sharp endotherm associated with the melting of the synthesized pure cocrystal at $T_{m,onset}$ = 125 °C, which demonstrates a decrease of the melting temperature compared to both parent compounds {T_m(NAP) = 155 °C and T_m[CBZ(III)] = 176 °C}. As is often the case with cocrystals obtained by grinding, and already observed in the case of carbamazepine, it was not possible to obtain a single crystal which would have facilitated the crystal structure determination (Roca-Paixão *et al.*, 2023; Guerain *et al.*, 2020).

2.2. Data collection

The powder X-ray diffraction patterns were measured at the high-resolution powder diffraction beamline CRISTAL at the Synchrotron SOLEIL in France. The beamline is equipped with a 1D detector 'MYTHEN2 X'. The selected energy was 18.4 keV, corresponding to a wavelength λ = 0.67132 Å, and a NIST standard LaB_6 660a sample was used for calibration. The cocrystal powder was enclosed in a borosilicate capillary (diameter 0.5 mm) and mounted on the goniometer head. The capillary was rotated during the experiments to reduce the effect of a possible preferential orientation. Data were

Table 1
Crystallographic data, profile and structural parameters for the CBZ:*S*-NAP cocrystal obtained after Rietveld refinement.

Crystal data	
Chemical formula	$C_{15}H_{12}N_2O{\cdot}C_{14}H_{14}O_3$
Molecular weight (g mol^{-1})	933.1
Crystal system, space group	orthorhombic, $P2_12_12_1$
Temperature (K)	293
a,b,c (Å)	33.5486 (9), 26.4223 (6), 5.36515 (10)
V (Å^3)	4755.83 (19)
Z	4
$F(000)$	1968
μ (mm^{-1})	0.077
Specimen shape, size (mm)	Cylinder, 0.5
2θ range (°)	1.5–20
Data collection	
Beamline	CRISTAL (SOLEIL)
Specimen mounting	0.5 mm diameter Lindemann capillary
Data collection mode	Transmission
Scan method	Continuous scan
Radiation type	Synchrotron 18.47 KeV, λ = 0.67132 Å
Binning size (°2θ)	0.004
Refinement	
R factors	R = 0.0413, $R_{wp,nb}$ = 0.0587, R_{exp} = 0.0168

collected at room temperature in the 1.5–50° 2θ range in less than 2 min to avoid radiation damage to the sample.

2.3. Structure solution and refinement

Regarding the indexation, the profiles of 20 reflections with a 2θ angle lower than 15° were refined individually with the program *DASH* (David *et al.*, 2006) in order to obtain their 2θ angular positions. The 2θ values of these reflections were computed in the program *DICVOL* (Boultif & Louër, 2004) and a unique orthorhombic cell was obtained: a = 33.564 ± 0.001, b = 26.444 ± 0.001, c = 5.3666 ± 0.001 Å and V = 4763.22 ± 0.2 Å^3. The calculated figures of merit are $M(20)$ = 19.2 and $F(20)$ = 136.3 (de Wolff *et al.*, 1968; Smith & Snyder, 1979).

Regarding the space-group determination, the *DASH* probabilistic approach (Markvardsen *et al.*, 2008), based on the systematic absences of Bragg peaks, was used. Eight individual peaks distributed over the whole 2θ range of the pattern were fitted to determine the peak-shape parameters, then the background, unit-cell and zero-point parameters were refined, and the most probable space group was calculated using Pawley refinement (Pawley, 1981). This method was repeated over ten times, each time on different sets of peaks. It led systematically to the space group $P2_12_12_1$, which is the most probable space group for an orthorhombic cell, according to the CSD.

Using this space group ($P2_12_12_1$) and the unit-cell parameters obtained previously, the X-ray diffraction pattern was refined using Pawley fitting (Pawley, 1981) with the program *DASH* (David *et al.*, 2006). The refinement was performed from 2θ = 1.5 to 15°. Again, eight individual peaks distributed over the whole 2θ range of the pattern were fitted to determine the peak-shape parameters. A five-term polynomial representing the background, the reflection intensities, the unit-cell parameters, the zero-point and the peak shape were refined. This led to a good correlation between the experimental diagram and the Pawley fitting to the profile, with χ^2 = 23.34. This result was used for the structure solution. In order to determine a hypothetical structural model, the simulated annealing algorithm of the program *DASH* was used (David *et al.*, 2006).

Here, the *S*-NAP molecule and the CBZ molecule were retrieved from the CSD, *i.e.* from the monoclinic *S*-NAP phase model (Tang *et al.*, 2015) and from the monoclinic CBZ phase model (Eccles *et al.*, 2011), respectively. The volume calculated from the indexation (V = 4763.22 Å^3) suggested the introduction of two molecules of CBZ and two molecules of *S*-NAP. The molecules were introduced randomly in the cell. The restraints options used for the calculations did not modify the bond lengths and angles. The translation and orientation

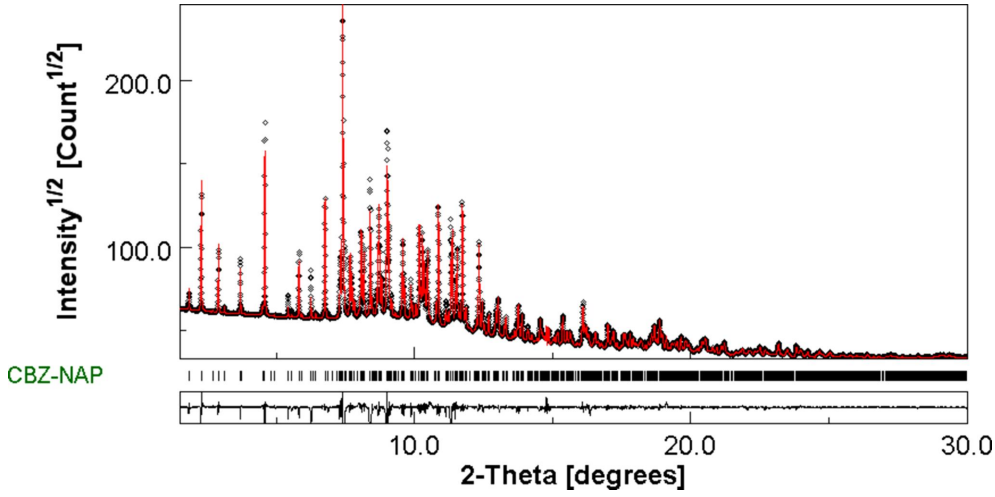

Figure 1
Final Rietveld plot of the CBZ:*S*-NAP cocrystal at room temperature. Observed intensities are indicated by dots, and solid lines represent the best-fit profile (upper trace) and the difference pattern (lower trace). The vertical bars correspond to the positions of the Bragg peaks.

parameters of the molecule in the cell, as well as the torsion angles, were defined as variables in the calculation. The maximum number of simulated annealing moves per run was fixed at 10 000 000 and led to the solution with a profile χ^2 factor close to 56.2. As a result, this structure was used for Rietveld refinement.

From this structural model, rigid-body Rietveld refinement was performed using *DASH*. The refinement was performed in three steps: first, the global isotropic temperature factor, second, the translation and orientation parameters of the molecule, and third, the five torsion angles. Strong restraints on the bond lengths and angles were applied. In particular, the naphthalene ring of the *S*-NAP molecules and the benzene rings of the CBZ molecules were kept planar. The lattice parameters and the background parameters were set free.

The structural model obtained from the simulated annealing was also minimized using periodic density functional theory with fixed-cell dispersion-corrected density functional theory (DFT-D) (Giannozzi *et al.*, 2009, 2017). In this minimization, the positions of the atoms were not constrained. The Perdew–Burke–Ernzerhof (PBE) function was used with projector-augmented wave pseudopotentials and the Grimme D3 correction, as implemented in the pw.x executable of the *Quantum Espresso* program (Giannozzi *et al.*, 2009, 2017). Overall, only tiny differences are found between the atomic positions determined from the DFT minimization and from the Rietveld method (see supporting information).

Atomic coordinates found at the end of the Rietveld refinement were introduced in the programs *JANA2020* (Petrícek *et al.*, 2014) and *MAUD* (Materials Analysis Using Diffraction; Lutterotti, 2010). *JANA2020* was used to generate the more accurate and complete CIF possible and *MAUD* was used to graphically compare the calculated and experimental X-ray diffraction diagram. One can see in Fig. 1 the very reasonable agreement found between the calculated and the experimental X-ray diffraction diagram, reinforcing the validity of the reported structure.

At the end of the Rietveld refinements, the lattice parameters were $a = 33.5486\ (9)$, $b = 26.4223\ (6)$, $c = 5.36515\ (10)$ Å and $V = 4755.83\ (19)$ Å^3. The final conventional Rietveld factors were $R = 0.0413$, $R_{wp} = 0.0587$, and $R_{exp} = 0.0168$. Such factors reflect the good correlation between the observed and simulated X-ray diffraction diagram, as shown in Fig. 1. Crystallographic data, profile and structural parameters are given in Table 1.

3. Discussion

The structure obtained for the title cocrystal has a large unit-cell volume (4755.83 Å^3), *i.e.* more than four times the unit-cell volume of commercial CBZ, and almost eight times the unit-cell volume of commercial *S*-NAP. This is related to the large lattice parameters *a* and *b*, of 33.5486 (9) and 26.4223 (6) Å, respectively.

Such lattice parameters are not surprising and are often obtained in the case of pharmaceutical cocrystals, such as ibuprofen–nicotinamide (Berry *et al.*, 2008), carbamazepine–indomethacine (Al Rahal *et al.*, 2020), carbamazepine–tartaric acid (Guerain *et al.*, 2020), naproxen–nicotinamide (Ando *et al.*, 2012; Neurohr *et al.*, 2015) and naproxen–isonicotinamide (Castro *et al.*, 2011).

It is closely related to the intricate arrangement of CBZ and *S*-NAP molecules within the crystal lattice (Fig. 2). The CBZ and *S*-NAP molecules are stacked without orientation change along the *c* direction, leading to a rather small *c* parameter of 5.36515 (10) Å. However, the molecular arrangement exhibits a greater complexity in the *a* and *b* directions. Along the *a* direction, an alternation pattern of CBZ and *S*-NAP molecules is observed, with a 180° rotation between two *S*-NAP molecules and a 180° rotation of the CBZ amine group between two CBZ molecules, *i.e.* an alternation of a total of four molecules (two CBZ and two *S*-NAP), contributing to a substantial large *a* unit-cell parameter [33.5486 (9) Å]. In the *b* direction, an alternation pattern of four molecules of either CBZ or *S*-NAP is observed. This alternation is attributed to the dimer formation between CBZ molecules, with each dimer experiencing a 180° rotation of the amine group. Such a dimer formation is commonly observed in cocrystals involving CBZ molecules (Roca-Paixão *et al.*, 2023; Walsh *et al.*, 2003; Al Rahal *et al.*, 2020; Habgood *et al.*, 2010; Oliveira *et al.*, 2011). As regards the *S*-NAP molecules, an inversion of the molecules two by two is observed, with, between two inversions, a 180° rotation of the carboxylic acid group. These two different conformations of the *S*-NAP molecules (by rotations of the groups along the C16—C17 and C30—C31 bonds) and the CBZ molecules (by rotations of the groups along the N1—C11 and N3—C54 bonds) are closely related to the complexity of the unit cell (see supporting information). As a consequence of these rotations, two symmetry-independent molecules (energetically different) can be distinguished, leading to a crystal symmetry lower than for a theoretical structure without those rotations. Such rotations facilitate the dimer formation (no steric hindrance) and break the symmetry, so the molecules forming the dimer are not identical.

This structural arrangement is linked to the hydrogen-bonding network of the cocrystal (Fig. 2). Notably, it is worth

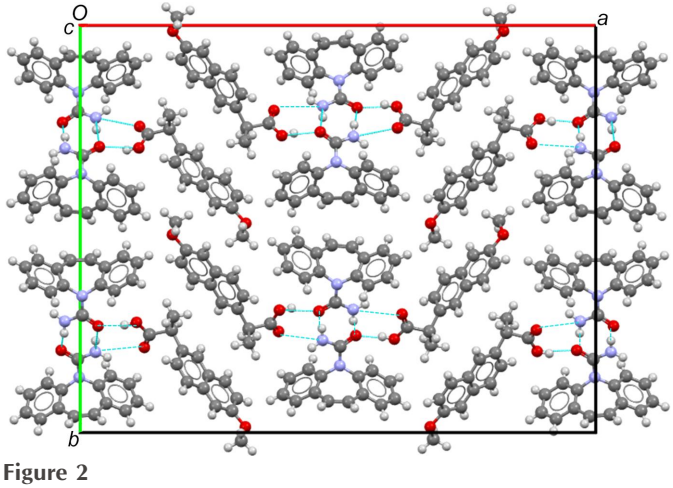

Figure 2
Visualization of the hydrogen-bond network of the CBZ:*S*-NAP cocrystal and projection of the unit cell along the [001] direction.

emphasizing that a single CBZ molecule interacts through three different hydrogen bonds, involving the two H atoms of its amine group and its O atom:

(i) with another CBZ molecule, with two N—H···O hydrogen bonds coming from one H atom of the amine group and forming a dimer as discussed previously;

(ii) with a *S*-NAP molecule, with an N—H···O hydrogen bond between the second H atom of the amine group and the carboxylic acid group of *S*-NAP;

(iii) with the same *S*-NAP molecule, with an O—H···O hydrogen bond between the O atoms of CBZ and the carboxylic acid group of *S*-NAP.

Consequently, the two *S*-NAP molecules also form a dimer which is based on the dimer of two CBZ molecules.

Also, the CBZ molecules are bound by hydrogen bonds of type (i), while the interactions between the two molecules composing the cocrystal are mainly related to hydrogen bonds of types (ii) and (iii), which bind the CBZ molecule to the *S*-NAP molecules. The whole forms a fairly rich and compact network of hydrogen bonds.

4. Conclusion

In this work, the cocrystal CBZ:*S*-NAP was synthesized by the liquid-assisted grinding in a 1:1 molar ratio. A search in the PDF-2, CSD and COD databases shows that the crystallographic structure of this cocrystal was unknown in the literature. It was solved using powder diffraction experiments at the beamline CRISTAL at the Synchrotron SOLEIL in France. Indexation of the diagram, simulated annealing, theoretical calculations and Rietveld refinement led to an orthorhombic cocrystal with the space group $P2_12_12_1$ (No. 19) and the following lattice parameters: a = 33.5486 (9), b = 26.4223 (6), c = 5.36515 (10) Å and V = 4755.83 (19) Å^3.

Acknowledgements

This project has received funding from the Interreg 2 Seas program 2014–2020 co-funded by the European Regional Development Fund (FEDER). The authors greatly acknowledge Florence Danède (MMT-UMET, Université de Lille) for performing the laboratory powder X-ray diffraction experiments.

Funding information

Funding for this research was provided by: European Regional Development Fund (FEDER) (subsidiary contract No. 2S01-059_IMODE).

References

Al Rahal, O., Majumder, M., Spillman, M. J., van de Streek, J. & Shankland, K. (2020). *Crystals*, **10**, 42.
Ando, S., Kikuchi, J., Fujimura, Y., Ida, Y., Higashi, K., Moribe, K. & Yamamoto, K. (2012). *J. Pharm. Sci.* **101**, 3214–3221.
Arlin, J. B., Price, L. S., Price, S. L. & Florence, A. J. (2011). *Chem. Commun.* **47**, 7074.
Berry, D. J., Seaton, C. C., Clegg, W., Harrington, R. W., Coles, S. J., Horton, P. N., Hursthouse, M. B., Storey, R., Jones, W., Friščić, T. & Blagden, N. (2008). *Cryst. Growth Des.* **8**, 1697–1712.
Boultif, A. & Louër, D. (2004). *J. Appl. Cryst.* **37**, 724–731.
Brittain, H. G. (2013). *J. Pharm. Sci.* **102**, 311–317.
Castro, R. A. E., Ribeiro, J. D. B., Maria, T. M. R., Ramos Silva, M., Yuste-Vivas, C., Canotilho, J. & Eusébio, M. E. S. (2011). *Cryst. Growth Des.* **11**, 5396–5404.
Childs, S. L., Wood, P. A., Rodríguez-Hornedo, N., Reddy, L. S. & Hardcastle, K. I. (2009). *Cryst. Growth Des.* **9**, 1869–1888.
Coe, W. J., Harrigan, P. E., O'Neill, T. B., Sands, B. S. & Watsky, J. E. (2003). Patent EA200200910 (A1).
David, W. I. F., Shankland, K., van de Streek, J., Pidcock, E., Motherwell, W. D. S. & Cole, J. C. (2006). *J. Appl. Cryst.* **39**, 910–915.
Degen, T., Sadki, M., Bron, E., König, U. & Nénert, G. (2014). *Powder Diffr.* **29**, S13–S18.
Drozd, K. V., Manin, A. N., Churakov, A. V. & Perlovich, G. L. (2017). *CrystEngComm*, **19**, 4273–4286.
Eccles, K. S., Stokes, S. P., Daly, C. A., Barry, N. M., McSweeney, S. P., O'Neill, D. J., Kelly, D. M., Jennings, W. B., Ní Dhubhghaill, O. M., Moynihan, H. A., Maguire, A. R. & Lawrence, S. E. (2011). *J. Appl. Cryst.* **44**, 213–215.
Fleischman, S. G., Kuduva, S. S., McMahon, J. A., Moulton, B., Bailey Walsh, R. D., Rodríguez-Hornedo, N. & Zaworotko, M. J. (2003). *Cryst. Growth Des.* **3**, 909–919.
Friščić, T. & Jones, W. (2010). *J. Pharm. Pharmacol.* **62**, 1547–1559.
Gates-Rector, S. & Blanton, T. (2019). *Powder Diffr.* **34**, 352–360.
Giannozzi, P., Andreussi, O., Brumme, T., Bunau, O., Nardelli, M. B., Calandra, M., Car, R., Cavazzoni, C., Ceresoli, D., Cococcioni, M., Colonna, N., Carnimeo, I., Corso, A. D., de Gironcoli, S., Delugas, P., DiStasio, R. A., Ferretti, A., Floris, A., Fratesi, G., Fugallo, G., Gebauer, R., Gerstmann, U., Giustino, F., Gorni, T., Jia, J., Kawamura, M., Ko, H.-Y., Kokalj, A., Küçükbenli, E., Lazzeri, M., Marsili, M., Marzari, N., Mauri, F., Nguyen, N. L., Nguyen, H.-V., Otero-de-la-Roza, A., Paulatto, L., Poncé, S., Rocca, D., Sabatini, R., Santra, B., Schlipf, M., Seitsonen, A. P., Smogunov, A., Timrov, I., Thonhauser, T., Umari, P., Vast, N., Wu, X. & Baroni, S. (2017). *J. Phys. Condens. Matter*, **29**, 465901.
Giannozzi, P., Baroni, S., Bonini, N., Calandra, M., Car, R., Cavazzoni, C., Ceresoli, D., Chiarotti, G. L., Cococcioni, M., Dabo, I., Corso, A. D., de Gironcoli, S., Fabris, S., Fratesi, G., Gebauer, R., Gerstmann, U., Gougoussis, C., Kokalj, A., Lazzeri, M., Martin-Samos, L., Marzari, N., Mauri, F., Mazzarello, R., Paolini, S., Pasquarello, A., Paulatto, L., Sbraccia, C., Scandolo, S., Sclauzero, G., Seitsonen, A. P., Smogunov, A., Umari, P. & Wentzcovitch, R. M. (2009). *J. Phys. Condens. Matter*, **21**, 395502.
Gražulis, S., Chateigner, D., Downs, R. T., Yokochi, A. F. T., Quirós, M., Lutterotti, L., Manakova, E., Butkus, J., Moeck, P. & Le Bail, A. (2009). *J. Appl. Cryst.* **42**, 726–729.
Groom, C. R., Bruno, I. J., Lightfoot, M. P. & Ward, S. C. (2016). *Acta Cryst.* B**72**, 171–179.
Grzesiak, A. L., Lang, M., Kim, K. & Matzger, A. J. (2003). *J. Pharm. Sci.* **92**, 2260–2271.
Guerain, M., Derollez, P., Roca-Paixão, L., Dejoie, C., Correia, N. T. & Affouard, F. (2020). *Acta Cryst.* C**76**, 225–230.
Habgood, M., Deij, M. A., Mazurek, J., Price, S. L. & ter Horst, J. H. (2010). *Cryst. Growth Des.* **10**, 903–912.
Lutterotti, L. (2010). *Nucl. Instrum. Methods Phys. Res. B*, **268**, 334–340.
Markvardsen, A. J., Shankland, K., David, W. I. F., Johnston, J. C., Ibberson, R. M., Tucker, M., Nowell, H. & Griffin, T. (2008). *J. Appl. Cryst.* **41**, 1177–1181.
Neurohr, C., Marchivie, M., Lecomte, S., Cartigny, Y., Couvrat, N., Sanselme, M. & Subra-Paternault, P. (2015). *Cryst. Growth Des.* **15**, 4616–4626.

Oliveira, M. A., Peterson, M. L. & Davey, R. J. (2011). *Cryst. Growth Des.* **11**, 449–457.
Oswald, I. D. H., Allan, D. R., McGregor, P. A., Motherwell, W. D. S., Parsons, S. & Pulham, C. R. (2002). *Acta Cryst.* B**58**, 1057–1066.
Pawley, G. S. (1981). *J. Appl. Cryst.* **14**, 357–361.
Petrícek, V., Dusek, M. & Palatinus, L. (2014). *Z. Kristallogr. Cryst. Mater.* **229**, 345–352.
Roca-Paixão, L., Correia, N. T. & Affouard, F. (2019). *CrystEngComm*, **21**, 6991–7001.
Roca-Paixão, L., Correia, N. T., Danède, F., Guerain, M. & Affouard, F. (2023). *Cryst. Growth Des.* **23**, 1355–1369.
Rustichelli, C., Gamberini, G., Ferioli, V., Gamberini, M. C., Ficarra, R. & Tommasini, S. (2000). *J. Pharm. Biomed. Anal.* **23**, 41–54.
Schultheiss, N. & Newman, A. (2009). *Cryst. Growth Des.* **9**, 2950–2967.
Smith, G. S. & Snyder, R. L. (1979). *J. Appl. Cryst.* **12**, 60–65.
Surov, A. O., Drozd, K. V., Ramazanova, A. G., Churakov, A. V., Vologzhanina, A. V., Kulikova, E. S. & Perlovich, G. L. (2023). *Pharmaceutics*, **15**, 1747.
Surov, A. O., Ramazanova, A. G., Voronin, A. P., Drozd, K. V., Churakov, A. V. & Perlovich, G. L. (2023). *Pharmaceutics*, **15**, 836.
Tang, G.-M., Wang, J.-H., Zhao, C., Wang, Y.-T., Cui, Y.-Z., Cheng, F.-Y. & Ng, S. W. (2015). *CrystEngComm*, **17**, 7258–7261.
Thakuria, R. & Sarma, B. (2018). *Crystals*, **8**, 101.
Tilborg, A., Springuel, G., Norberg, B., Wouters, J. & Leyssens, T. (2013). *CrystEngComm*, **15**, 3341–3350.
Tumanova, N., Tumanov, N., Fischer, F., Morelle, F., Ban, V., Robeyns, K., Filinchuk, Y., Wouters, J., Emmerling, F. & Leyssens, T. (2018). *CrystEngComm*, **20**, 7308–7321.
Vishweshwar, P., McMahon, J. A., Bis, J. A. & Zaworotko, M. J. (2006). *J. Pharm. Sci.* **95**, 499–516.
Walsh, R. D. B., Bradner, M. W., Fleischman, S., Morales, L. A., Moulton, B., Rodríguez-Hornedo, N. & Zaworotko, M. J. (2003). *Chem. Commun.* pp. 186–187.
Wolff, P. M. de (1968). *J. Appl. Cryst.* **1**, 108–113.

supporting information

Acta Cryst. (2024). C**80**, 37-42 [https://doi.org/10.1107/S2053229624000639]

Using synchrotron high-resolution powder X-ray diffraction for the structure determination of a new cocrystal formed by two active principle ingredients

Mathieu Guerain, Natalia T. Correia, Luisa Roca-Paixão, Hubert Chevreau and Frederic Affouard

Computing details

2-Azatricyclo[9.4.0.0^{3,8}]pentadeca-1(11),3,5,7,9,12,14-heptaene-2-carboxamide; (2*S*)-2-(6-methoxynaphthalen-2-yl)propanoic acid

Crystal data

$C_{15}H_{12}N_2O{\cdot}C_{14}H_{14}O_3$
M_r = 933.1
Orthorhombic, $P2_12_12_1$
Hall symbol: P 2xab;2ybc;2zac
a = 33.5486 (9) Å
b = 26.4223 (6) Å
c = 5.36515 (10) Å
V = 4755.83 (19) Å^3
Z = 4
F(000) = 1968
D_x = 1.303 Mg m^{-3}
Synchrotron radiation
T = 293 K
white

Data collection

Synchrotron diffractometer
Radiation source: synchrotron, synchrotron
$2\theta_{min}$ = 1.5°, $2\theta_{max}$ = 20°, $2\theta_{step}$ = 0.004°

Refinement

R_p = 0.041
R_{wp} = 0.059
R_{exp} = 0.017
$R(F)$ = 0.061
4626 data points
Profile function: Pseudo-Voigt
18 parameters
0 restraints
0 constraints
H-atom parameters constrained
Weighting scheme based on measured s.u.'s
$(\Delta/\sigma)_{max}$ < 0.001
Background function: 8 Legendre polynoms
Preferred orientation correction: none

Fractional atomic coordinates and isotropic or equivalent isotropic displacement parameters (Å^2)

	x	*y*	*z*	U_{iso}*/U_{eq}
O1	−0.03708	0.79805	−0.75688	0.0204*
N1	−0.00202	0.86426	−0.5944	0.0204*
N2	0.02941	0.80227	−0.82658	0.0204*
H1	0.05247	0.8151	−0.80009	0.0407*
H2	0.02947	0.77446	−0.91061	0.0407*
C1	0.09551	0.88081	−0.27503	0.0204*
H3	0.11052	0.86493	−0.15204	0.0407*

C2	0.05877	0.86144	−0.34163	0.0204*
H4	0.04911	0.83264	−0.26252	0.0407*
C3	0.03627	0.88458	−0.52524	0.0204*
C4	−0.03623	0.89535	−0.54339	0.0204*
C5	−0.04183	0.94031	−0.67733	0.0204*
C6	−0.07707	0.96705	−0.63353	0.0204*
H5	−0.08178	0.99679	−0.72138	0.0407*
C7	−0.10505	0.95055	−0.46369	0.0204*
H6	−0.12832	0.96902	−0.43898	0.0407*
C8	0.10994	0.92362	−0.39067	0.0204*
H7	0.13461	0.93678	−0.34574	0.0407*
C9	0.08768	0.94677	−0.5727	0.0204*
H8	0.09776	0.97546	−0.65081	0.0407*
C10	0.05023	0.92835	−0.64399	0.0204*
C11	−0.0049	0.8199	−0.72844	0.0204*
C12	−0.06406	0.87937	−0.36864	0.0204*
H9	−0.05944	0.85009	−0.27671	0.0407*
C13	−0.09858	0.90685	−0.33082	0.0204*
H10	−0.11738	0.89579	−0.21586	0.0407*
C14	−0.01222	0.96034	−0.85026	0.0204*
H11	−0.02189	0.97839	−0.98618	0.0407*
C15	0.02731	0.95543	−0.83354	0.0204*
H12	0.04209	0.97122	−0.95782	0.0407*
O2	0.61529	0.25182	0.44673	0.0204*
O3	0.61376	0.1993	0.77426	0.0204*
H13	0.59031	0.19419	0.72567	0.0407*
O4	0.82124	0.014	0.82723	0.0204*
C16	0.63113	0.23257	0.62617	0.0204*
C17	0.673	0.24546	0.71131	0.0204*
H14	0.68691	0.26376	0.57338	0.0407*
C18	0.69468	0.19532	0.75826	0.0204*
C19	0.72531	0.18057	0.60479	0.0204*
H15	0.73189	0.20069	0.46404	0.0407*
C20	0.74722	0.13579	0.65344	0.0204*
C21	0.78048	0.12168	0.50486	0.0204*
H16	0.78657	0.14036	0.35857	0.0407*
C22	0.80374	0.08152	0.57065	0.0204*
H17	0.82634	0.07313	0.4724	0.0407*
C23	0.79456	0.05221	0.78338	0.0204*
C24	0.76167	0.063	0.92521	0.0204*
H18	0.755	0.04225	1.06351	0.0407*
C25	0.7375	0.1057	0.86336	0.0204*
C26	0.70467	0.12065	1.01286	0.0204*
H19	0.69689	0.10019	1.15002	0.0407*
C27	0.68404	0.16424	0.96221	0.0204*
H20	0.66229	0.17368	1.06554	0.0407*
C28	0.67241	0.27958	0.94087	0.0204*
H21	0.65965	0.31184	0.89884	0.0407*

H22	0.69978	0.2858	0.99658	0.0407*
H23	0.65738	0.263	1.07453	0.0407*
C29	0.81518	−0.01618	1.04426	0.0204*
H24	0.81497	0.00558	1.19192	0.0407*
H25	0.8368	−0.04094	1.0588	0.0407*
H26	0.78963	−0.03393	1.03096	0.0407*
O5	0.12427	0.79096	0.99754	0.0204*
O6	0.10916	0.72942	0.72646	0.0204*
H27	0.08578	0.73546	0.77371	0.0407*
O7	0.32033	0.98612	0.7212	0.0204*
C30	0.1342	0.75939	0.84598	0.0204*
C31	0.17724	0.74861	0.7784	0.0204*
H28	0.19015	0.73071	0.92129	0.0407*
C32	0.1979	0.79981	0.74249	0.0204*
C33	0.22754	0.81472	0.90301	0.0204*
H29	0.23403	0.79397	1.04171	0.0407*
C34	0.24857	0.86058	0.86465	0.0204*
C35	0.28087	0.87499	1.02061	0.0204*
H30	0.28681	0.85563	1.16499	0.0407*
C36	0.30342	0.9164	0.96465	0.0204*
H31	0.32541	0.925	1.06774	0.0407*
C37	0.2944	0.94667	0.75497	0.0204*
C38	0.26236	0.93556	0.60631	0.0204*
H32	0.25576	0.95692	0.47013	0.0407*
C39	0.23898	0.89161	0.65781	0.0204*
C40	0.20713	0.8764	0.50086	0.0204*
H33	0.19942	0.89741	0.36561	0.0407*
C41	0.18735	0.83175	0.54162	0.0204*
H34	0.16625	0.82216	0.43343	0.0407*
C42	0.18014	0.71492	0.54795	0.0204*
H35	0.16791	0.68202	0.58336	0.0407*
H36	0.20821	0.71008	0.50379	0.0407*
H37	0.16612	0.73106	0.40878	0.0407*
C43	0.31238	1.02005	0.52057	0.0204*
H38	0.31132	1.00109	0.36392	0.0407*
H39	0.3336	1.04545	0.51129	0.0407*
H40	0.28677	1.03691	0.54886	0.0407*
O8	0.46553	0.26164	0.21291	0.0204*
N3	0.4964	0.33546	0.10608	0.0204*
N4	0.52998	0.27322	0.32447	0.0204*
H41	0.55079	0.29173	0.34056	0.0407*
H42	0.53123	0.24423	0.39775	0.0407*
C44	0.3987	0.37502	−0.15742	0.0204*
H43	0.38096	0.36459	−0.28034	0.0407*
C45	0.43356	0.34836	−0.11794	0.0204*
H44	0.43924	0.32013	−0.21514	0.0407*
C46	0.46007	0.36336	0.06524	0.0204*
C47	0.53309	0.36155	0.05497	0.0204*

C48	0.54479	0.40195	0.20748	0.0204*
C49	0.58211	0.42343	0.1609	0.0204*
H45	0.59083	0.45001	0.26057	0.0407*
C50	0.60635	0.40632	−0.02873	0.0204*
H46	0.63112	0.42121	−0.05492	0.0407*
C51	0.39018	0.41702	−0.01484	0.0204*
H47	0.36678	0.43508	−0.04149	0.0407*
C52	0.41644	0.4321	0.16689	0.0204*
H48	0.41033	0.4603	0.26322	0.0407*
C53	0.45216	0.40616	0.21116	0.0204*
C54	0.49572	0.28829	0.21582	0.0204*
C55	0.5572	0.34508	−0.1392	0.0204*
H49	0.54858	0.31904	−0.24273	0.0407*
C56	0.59395	0.36727	−0.17914	0.0204*
H50	0.61023	0.35582	−0.30739	0.0407*
C57	0.51934	0.42275	0.40268	0.0204*
H51	0.53216	0.43591	0.54197	0.0407*
C58	0.47957	0.42484	0.40198	0.0204*
H52	0.46785	0.44008	0.53995	0.0407*

Atomic displacement parameters (Å²)

	U^{11}	U^{22}	U^{33}	U^{12}	U^{13}	U^{23}
?	?	?	?	?	?	?

Geometric parameters (Å, º)

O1—C11	1.2337 (1)	O5—C30	1.2116 (1)
N1—C3	1.4409 (1)	O6—H27	0.8396 (1)
N1—C4	1.4377 (1)	O6—C30	1.3206 (1)
N1—C11	1.3785 (1)	O7—C37	1.3697 (1)
N2—H1	0.8565 (1)	O7—C43	1.4260 (1)
N2—H2	0.8621 (1)	C30—C31	1.5158 (1)
N2—C11	1.3488 (1)	C31—H28	0.9995 (1)
C1—H3	0.9301 (1)	C31—C32	1.5322 (1)
C1—C2	1.3816 (1)	C31—C42	1.5266 (1)
C1—C8	1.3780 (1)	C32—C33	1.3732 (1)
C2—H4	0.9296 (1)	C32—C41	1.4138 (1)
C2—C3	1.3835 (1)	C33—H29	0.9496 (1)
C3—C10	1.4010 (1)	C33—C34	1.4172 (1)
C4—C5	1.4010 (1)	C34—C35	1.4210 (1)
C4—C12	1.3889 (1)	C34—C39	1.4168 (1)
C5—C6	1.3972 (1)	C35—H30	0.9494 (1)
C5—C14	1.4587 (1)	C35—C36	1.3637 (1)
C6—H5	0.9298 (1)	C36—H31	0.9496 (1)
C6—C7	1.3790 (1)	C36—C37	1.4131 (1)
C7—H6	0.9302 (1)	C37—C38	1.3703 (1)
C7—C13	1.3742 (1)	C38—H32	0.9494 (1)

C8—H7	0.9295 (1)	C38—C39	1.4283 (1)
C8—C9	1.3732 (1)	C39—C40	1.4186 (1)
C9—H8	0.9299 (1)	C40—H33	0.9495 (1)
C9—C10	1.4006 (1)	C40—C41	1.3711 (1)
C10—C15	1.4620 (1)	C41—H34	0.9499 (1)
C12—H9	0.9305 (1)	C42—H35	0.9799 (1)
C12—C13	1.3819 (1)	C42—H36	0.9794 (1)
C13—H10	0.9293 (1)	C42—H37	0.9801 (1)
C14—H11	0.9298 (1)	C43—H38	0.9791 (1)
C14—C15	1.3355 (1)	C43—H39	0.9796 (1)
C15—H12	0.9298 (1)	C43—H40	0.9796 (1)
O2—C16	1.2116 (1)	O8—C54	1.2337 (1)
O3—H13	0.8397 (1)	N3—C46	1.4412 (1)
O3—C16	1.3205 (1)	N3—C47	1.4372 (1)
O4—C23	1.3696 (1)	N3—C54	1.3786 (1)
O4—C29	1.4259 (1)	N4—H41	0.8568 (1)
C16—C17	1.5158 (1)	N4—H42	0.8620 (1)
C17—H14	0.9996 (1)	N4—C54	1.3489 (1)
C17—C18	1.5322 (1)	C44—H43	0.9301 (1)
C17—C28	1.5265 (1)	C44—C45	1.3816 (1)
C18—C19	1.3733 (1)	C44—C51	1.3778 (1)
C18—C27	1.4139 (1)	C45—H44	0.9299 (1)
C19—H15	0.9495 (1)	C45—C46	1.3835 (1)
C19—C20	1.4172 (1)	C46—C53	1.4008 (1)
C20—C21	1.4211 (1)	C47—C48	1.4011 (1)
C20—C25	1.4166 (1)	C47—C55	1.3888 (1)
C21—H16	0.9494 (1)	C48—C49	1.3972 (1)
C21—C22	1.3636 (1)	C48—C57	1.4587 (1)
C22—H17	0.9497 (1)	C49—H45	0.9299 (1)
C22—C23	1.4132 (1)	C49—C50	1.3787 (1)
C23—C24	1.3703 (1)	C50—H46	0.9301 (1)
C24—H18	0.9493 (1)	C50—C56	1.3744 (1)
C24—C25	1.4285 (1)	C51—H47	0.9298 (1)
C25—C26	1.4186 (1)	C51—C52	1.3732 (1)
C26—H19	0.9497 (1)	C52—H48	0.9297 (1)
C26—C27	1.3709 (1)	C52—C53	1.4008 (1)
C27—H20	0.9497 (1)	C53—C58	1.4620 (1)
C28—H21	0.9801 (1)	C55—H49	0.9304 (1)
C28—H22	0.9795 (1)	C55—C56	1.3819 (1)
C28—H23	0.9800 (1)	C56—H50	0.9291 (1)
C29—H24	0.9789 (1)	C57—H51	0.9297 (1)
C29—H25	0.9799 (1)	C57—C58	1.3354 (1)
C29—H26	0.9797 (1)	C58—H52	0.9299 (1)

C3—N1—C4	116.7294 (16)	H27—O6—C30	109.4922 (14)
C3—N1—C11	120.9078 (6)	C37—O7—C43	117.3545 (10)
C4—N1—C11	121.9500 (10)	O5—C30—O6	124.3195 (13)
H1—N2—H2	114.9620 (7)	O5—C30—C31	123.49

H1—N2—C11	124.7054 (14)	O6—C30—C31	112.1571 (13)
H2—N2—C11	120.0349 (7)	C30—C31—H28	108.5568 (10)
H3—C1—C2	119.9594 (10)	C30—C31—C32	107.1631 (11)
H3—C1—C8	119.9702 (12)	C30—C31—C42	111.3469 (4)
C2—C1—C8	120.0704 (6)	H28—C31—C32	108.5553 (11)
C1—C2—H4	119.7453 (6)	H28—C31—C42	108.5216 (14)
C1—C2—C3	120.4772 (10)	C32—C31—C42	112.5920 (10)
H4—C2—C3	119.7775 (12)	C31—C32—C33	120.1333 (7)
N1—C3—C2	120.3393 (10)	C31—C32—C41	120.6391 (9)
N1—C3—C10	119.2435 (6)	C33—C32—C41	119.2148 (10)
C2—C3—C10	120.4130 (11)	C32—C33—H29	119.4628 (10)
N1—C4—C5	119.5966 (8)	C32—C33—C34	120.9788 (8)
N1—C4—C12	119.4354 (12)	H29—C33—C34	119.5584 (9)
C5—C4—C12	120.9213 (9)	C33—C34—C35	121.5477 (7)
C4—C5—C6	117.1273 (7)	C33—C34—C39	119.7029 (9)
C4—C5—C14	122.8582 (9)	C35—C34—C39	118.6419 (9)
C6—C5—C14	119.9841 (13)	C34—C35—H30	119.7430 (9)
C5—C6—H5	119.0707 (7)	C34—C35—C36	120.5557 (9)
C5—C6—C7	121.8213 (12)	H30—C35—C36	119.7012 (9)
H5—C6—C7	119.1080 (9)	C35—C36—H31	119.6524 (9)
C6—C7—H6	119.9758 (12)	C35—C36—C37	120.7039 (9)
C6—C7—C13	120.0598 (9)	H31—C36—C37	119.6437 (9)
H6—C7—C13	119.9644 (7)	O7—C37—C36	113.5800 (10)
C1—C8—H7	120.2072 (6)	O7—C37—C38	125.7488 (9)
C1—C8—C9	119.6576 (12)	C36—C37—C38	120.6709 (8)
H7—C8—C9	120.1352 (10)	C37—C38—H32	120.2332 (9)
C8—C9—H8	119.0709 (12)	C37—C38—C39	119.4948 (9)
C8—C9—C10	121.8215 (10)	H32—C38—C39	120.2720 (10)
H8—C9—C10	119.1076 (6)	C34—C39—C38	119.8226 (10)
C3—C10—C9	117.5511 (6)	C34—C39—C40	118.1683 (10)
C3—C10—C15	122.9915 (11)	C38—C39—C40	121.9480 (9)
C9—C10—C15	119.4513 (10)	C39—C40—H33	119.5503 (10)
O1—C11—N1	121.5827 (7)	C39—C40—C41	120.9065 (7)
O1—C11—N2	122.4722 (14)	H33—C40—C41	119.5432 (10)
N1—C11—N2	115.9442 (8)	C32—C41—C40	120.9313 (10)
C4—C12—H9	119.9074 (9)	C32—C41—H34	119.5473 (10)
C4—C12—C13	120.1830 (12)	C40—C41—H34	119.5213 (8)
H9—C12—C13	119.9097 (7)	C31—C42—H35	109.4871 (11)
C7—C13—C12	119.8468 (7)	C31—C42—H36	109.4705 (3)
C7—C13—H10	120.0860 (9)	C31—C42—H37	109.4327 (13)
C12—C13—H10	120.0672 (12)	H35—C42—H36	109.4918 (10)
C5—C14—H11	116.5743 (14)	H35—C42—H37	109.4372 (10)
C5—C14—C15	126.7471 (10)	H36—C42—H37	109.5081 (11)
H11—C14—C15	116.6787 (4)	O7—C43—H38	109.4555 (15)
C10—C15—C14	128.0632 (6)	O7—C43—H39	109.4594 (11)
C10—C15—H12	115.9733 (15)	O7—C43—H40	109.4493 (7)
C14—C15—H12	115.9634 (10)	H38—C43—H39	109.4692 (7)
H13—O3—C16	109.4938 (10)	H38—C43—H40	109.5010 (7)

C23—O4—C29	117.3454 (9)	H39—C43—H40	109.4929 (17)
O2—C16—O3	124.3346 (12)	C46—N3—C47	116.7413 (17)
O2—C16—C17	123.4746 (6)	C46—N3—C54	120.8892 (9)
O3—C16—C17	112.1610 (9)	C47—N3—C54	121.9580 (8)
C16—C17—H14	108.5547 (11)	H41—N4—H42	114.9388 (10)
C16—C17—C18	107.1671 (12)	H41—N4—C54	124.7071 (14)
C16—C17—C28	111.3352 (6)	H42—N4—C54	120.0579 (6)
H14—C17—C18	108.5630 (11)	H43—C44—C45	119.9531 (11)
H14—C17—C28	108.5233 (14)	H43—C44—C51	119.9712 (10)
C18—C17—C28	112.5927 (10)	C45—C44—C51	120.0757 (7)
C17—C18—C19	120.1347 (7)	C44—C45—H44	119.7674 (7)
C17—C18—C27	120.6362 (9)	C44—C45—C46	120.4658 (11)
C19—C18—C27	119.2163 (10)	H44—C45—C46	119.7668 (10)
C18—C19—H15	119.4671 (9)	N3—C46—C45	120.3412 (11)
C18—C19—C20	120.9729 (8)	N3—C46—C53	119.2222 (7)
H15—C19—C20	119.5600 (9)	C45—C46—C53	120.4324 (10)
C19—C20—C21	121.5319 (8)	N3—C47—C48	119.6008 (7)
C19—C20—C25	119.7090 (9)	N3—C47—C55	119.4473 (10)
C21—C20—C25	118.6503 (9)	C48—C47—C55	120.9050 (11)
C20—C21—H16	119.7563 (8)	C47—C48—C49	117.1338 (6)
C20—C21—C22	120.5488 (10)	C47—C48—C57	122.8436 (11)
H16—C21—C22	119.6949 (9)	C49—C48—C57	119.9922 (11)
C21—C22—H17	119.6596 (10)	C48—C49—H45	119.0668 (6)
C21—C22—C23	120.7144 (10)	C48—C49—C50	121.8271 (10)
H17—C22—C23	119.6260 (8)	H45—C49—C50	119.1061 (12)
O4—C23—C22	113.5941 (10)	C49—C50—H46	119.9854 (10)
O4—C23—C24	125.7472 (9)	C49—C50—C56	120.0613 (11)
C22—C23—C24	120.6585 (8)	H46—C50—C56	119.9533 (6)
C23—C24—H18	120.2427 (8)	C44—C51—H47	120.2096 (7)
C23—C24—C25	119.4986 (9)	C44—C51—C52	119.6588 (10)
H18—C24—C25	120.2587 (10)	H47—C51—C52	120.1316 (11)
C20—C25—C24	119.8201 (10)	C51—C52—H48	119.0669 (10)
C20—C25—C26	118.1607 (9)	C51—C52—C53	121.8217 (11)
C24—C25—C26	121.9581 (9)	H48—C52—C53	119.1114 (7)
C25—C26—H19	119.5374 (9)	C46—C53—C52	117.5364 (7)
C25—C26—C27	120.9190 (8)	C46—C53—C58	123.0090 (10)
H19—C26—C27	119.5436 (10)	C52—C53—C58	119.4486 (11)
C18—C27—C26	120.9244 (10)	O8—C54—N3	121.6149 (9)
C18—C27—H20	119.5496 (9)	O8—C54—N4	122.4495 (14)
C26—C27—H20	119.5260 (8)	N3—C54—N4	115.9347 (7)
C17—C28—H21	109.4910 (11)	C47—C55—H49	119.9024 (12)
C17—C28—H22	109.4595 (6)	C47—C55—C56	120.1963 (10)
C17—C28—H23	109.4549 (13)	H49—C55—C56	119.9013 (6)
H21—C28—H22	109.4942 (10)	C50—C56—C55	119.8360 (6)
H21—C28—H23	109.4135 (11)	C50—C56—H50	120.0894 (11)
H22—C28—H23	109.5143 (12)	C55—C56—H50	120.0746 (10)
O4—C29—H24	109.4783 (16)	C48—C57—H51	116.5660 (15)
O4—C29—H25	109.4424 (9)	C48—C57—C58	126.7540 (8)

O4—C29—H26	109.4512 (6)	H51—C57—C58	116.6800 (7)
H24—C29—H25	109.4533 (8)	C53—C58—C57	128.0583 (9)
H24—C29—H26	109.5011 (7)	C53—C58—H52	115.9562 (15)
H25—C29—H26	109.5010 (18)	C57—C58—H52	115.9855 (6)

Hydrogen-bond geometry (Å, º)

D—H···*A*	*D*—H	H···*A*	*D*···*A*	*D*—H···*A*
N2—H2···O8^{i}	0.86	2.24	2.9975	146.58
C1—H3···O5^{ii}	0.93	2.16	2.9505	141.86
O3—H13···O1^{iii}	0.84	1.80	2.5789	153.52
C28—H23···O2^{iv}	0.98	2.46	3.4024	160.33
O6—H27···O8^{v}	0.84	1.75	2.5179	150.36
N4—H41···O2	0.86	2.47	2.9902	119.52
N4—H42···O1^{iii}	0.86	2.17	2.9407	148.25
C51—H47···O4^{vi}	0.93	2.34	3.1120	140.49

Symmetry codes: (i) −*x*+1/2, −*y*+1, *z*−3/2; (ii) *x*, *y*, *z*−1; (iii) −*x*+1/2, −*y*+1, *z*+3/2; (iv) *x*, *y*, *z*+1; (v) −*x*+1/2, −*y*+1, *z*+1/2; (vi) *x*−1/2, −*y*+1/2, −*z*+1.